Inertial effects in Büttiker-Landauer motor and refrigerator at the overdamped limit

Ronald Benjamin and Ryoichi Kawai[*]

Department of Physics, University of Alabama at Birmingham, Birmingham, Alabama 35294, USA
(Received 28 March 2008; published 29 May 2008)

We investigate the energetics of a Brownian motor driven by position-dependent temperature, commonly known as the Büttiker-Landauer motor. Overdamped models ($M=0$) predict that the motor can attain Carnot efficiency. However, the overdamped limit ($M \rightarrow 0$) contradicts the previous prediction due to the kinetic energy contribution to the heat transfer. Using molecular dynamics simulation and numerical solution of the inertial Langevin equation, we confirm that the motor can never achieve Carnot efficiency and verify that the heat flow via kinetic energy diverges as $M^{-1/2}$ in the overdamped limit. The reciprocal process of the motor, namely, the Büttiker-Landauer refrigerator, is also examined. In this case, the overdamped approach succeeds in predicting the heat transfer only when there is no temperature gradient. Its found that the Onsager symmetry between the motor and refrigerator does not suffer from the singular behavior of the kinetic energy contribution.

I. INTRODUCTION

Since the industrial revolution, thermodynamics has been a guiding principle for the development of new technology. We are now entering the era of nanotechnology, where we can construct and manipulate nanoscale objects as we desire. Realization of nanoscale machines is within our reach. However, we still have to overcome various issues. As the size of a system approaches that of molecules, thermal fluctuations begin to play a significant role. It would be rather difficult to operate a nanomachine against strong thermal fluctuations. Instead, the nanomachine must be able to work harmoniously or even collaboratively with the fluctuations. In order to design such machines, we need to understand thermodynamics of small systems, taking into account large thermal fluctuations. Furthermore, the molecular machinery in biological systems such as motor proteins is similarly subject to large thermal fluctuations. Thermodynamics, at the macromolecular level, is also essential in the investigation of such biological machines.

Unfortunately, since it was originally developed for macroscopic systems where fluctuations are negligible, standard thermodynamics is often powerless in cases where fluctuations dominate. We often resort to stochastic approaches such as the Fokker-Planck or Langevin equation. Despite the fact that these approaches have been successfully used for many years, the relation between thermodynamics and stochastic methods is not well established. It was only ten years ago that a general theory of energetics such as heat within the stochastic regime (stochastic energetics) [1–3] was developed. The validity of the theory needs to be systematically tested with experiments or first-principles simulations.

When traditional thermodynamics was developed, the Carnot engine played a key role as an idealized model. Similarly, Brownian motors [4] have been basic working models for systems dominated by thermal fluctuations. In particular, autonomous thermal engines such as the Feynman-Smoluchowski (FS) [5] and Büttiker-Landauer (BL) motors [6,7], unlike other Brownian motors, do not require a time-dependent external influence. These motors are driven solely by thermal fluctuations and their motility disappears when the motors become macroscopic in size.

There is no difficulty in the investigation of their motility using standard stochastic approaches. However, it was not straightforward to investigate the thermodynamics of these systems. In his celebrated textbook [5], Feynman attempted to investigate the thermodynamics of the FS motor and concluded that it can reach Carnot efficiency. Yet he overlooked the effect of fluctuations, and later it was shown that the heat transfer between two heat reservoirs never ceases even when the motor moves quasistatically, and thus it is not possible to reach the Carnot efficiency [1,8,9]. Even when the average velocity of the motor is zero, fluctuations around the mean value can transport some energy. It is this fluctuation that transports heat. Recently, a simpler model of the FS motor was developed and the result confirms the presence of such heat transfer [10]. Similar heat transfer was investigated in the problems of adiabatic [11] and shared pistons [12]. The reverse process of the FS motor, namely, the FS refrigerator, has also been studied using various models [13–15].

The BL motor is just an overdamped Brownian particle in a periodic potential field subject to a spatially inhomogeneous temperature. When the temperature changes across a potential barrier, the Brownian particle jumps over the barrier more often from the hot side to the cold side than the other way [6,7,16]. Therefore, Brownian particles move in one direction on average. Whereas the FS motor is simultaneously in contact with two heat baths, the BL motor moves from one heat bath to another by itself. Therefore, the BL motor is a different class of Brownian motor from the FS motor. In order for the BL motor to operate continuously, it must be thermalized with the local environment before entering the next heat bath. Thus, it works better in the overdamped limit but fails in the underdamped limit [17].

As for the FS motor, there is no difficulty in explaining the motility of the BL motor. However, the thermodynamics of this system is not straightforward. Intuitively, we expect nonvanishing heat transfer even when the average current is

zero since the Brownian particles can move back and forth between the hot and cold regions by thermal fluctuations [18,19]. Despite this anticipation, some previous investigation claimed that the BL motor can reach Carnot efficiency [20,21] and under certain conditions can act as a refrigerator, attaining the corresponding Carnot coefficient of performance [21]. It turns out, however, that the overdamped Langevin approach fails to predict such heat transfer for the BL motor while it works fine for the FS motor [1,9]. It appears that, even when the system is in the overdamped regime, the inertial mass (M) apparently plays a critical role in certain thermodynamic processes. In fact, the heat evaluated by assuming $M=0$ at the beginning does not agree with the result obtained by taking the limit $M \to 0$ at the end. This singularity has been phenomenologically predicted [18,19] but not yet experimentally tested. Due to the lack of experimental confirmation, this issue is still a subject of debate [21,22].

In this paper, we investigate the BL motor and its reciprocal process, the BL refrigerator, using stochastic energetics based on the Langevin approach, with and without inertial effects, and compare the results with molecular dynamics simulation. Our main objective is to check the failure of the overdamped Langevin method and the validity of the inertial Langevin method by comparing the results with molecular dynamics simulations. The overdamped method appears to fail for the BL motor involving inhomogeneous temperature but works fine for the BL refrigerator operated with homogeneous temperature. On the other hand, these two processes are related to one another through Onsager's symmetry, which is not obvious for a system with inhomogeneous temperature, prompting us to investigate the validity of the Onsager symmetry in the overdamped regime [23]. We will check the validity numerically, taking into account inertial effects.

In the next section, we introduce a concrete model of the BL motor and/or refrigerator which can be investigated by both Langevin and molecular dynamics simulations. In Sec. III, a brief heuristic discussion based on the overdamped Langevin equation is given. In Sec. IV the results of the overdamped approach are compared with numerical simulations of the Langevin equation, taking inertia into account, and with molecular dynamics simulations. Further discussion and conclusions follow in the final section.

II. THE MODEL AND METHODS

A. The model

We consider a chain of two-dimensional cells aligned in the x direction as illustrated in Fig. 1. Each cell has a width of $L/2$ and is filled with N gas particles confined in the cell they belong to. No direct heat exchange between cells through the walls is permitted. The gas particles in each cell act as a heat reservoir with their own temperature, independent of the temperature in other cells. Brownian particles of mass M are placed in the cells. Unlike the gas particles, the Brownian particles are allowed to move freely from one cell to another through the walls, and they are also subject to a potential field $U(x)$, which is periodic in the x direction with
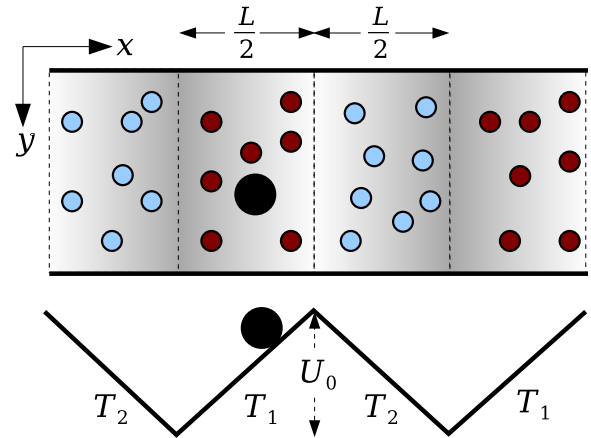

FIG. 1. (Color online) Two rectangular reservoirs filled with gas particles at temperatures T_1 and T_2 are alternately connected. Gas particles [red (dark gray) and blue (light gray) circles] are confined in the cell and only Brownian particles (large black circle) can move through the walls. Brownian particles are subjected to a piecewise-linear potential as shown at the bottom.

a periodicity L and constant in the y direction. For simplicity, we use a piecewise-linear potential

$$U(x) = \begin{cases} \dfrac{2U_0}{L}x & \text{for } 0 < x \le \frac{L}{2}, \\[2mm] \dfrac{2U_0}{L}(L-x) & \text{for } \frac{L}{2} < x \le L, \end{cases} \tag{1}$$

where U_0 is the potential height. The x coordinate is chosen such that the location of potential maxima or minima coincide with the cell boundaries as shown in Fig. 1. In addition to the periodic potential, a constant external force F is exerted on the Brownian particles. We further assume that temperature is periodic with the same periodicity as the potential and piecewise constant,

$$T(x) = \begin{cases} T_1 & \text{for } 0 < x \le \frac{L}{2}, \\[2mm] T_2 & \text{for } \frac{L}{2} < x \le L. \end{cases} \tag{2}$$

Temperature is measured in energy units ($k_B=1$).

For technical simplicity, we consider only two cells (cell 1 for $0 \le x < L/2$ and cell 2 for $L/2 \le x < L$) with a periodic boundary condition instead of infinitely long chains.

B. Langevin approaches

Molecular dynamics (MD) simulation is a useful tool to investigate this kind of model. However, a simpler mathematical model is desirable since MD simulation is computationally quite demanding. Apart from long-time fluid dynamical effects in two dimensions, the motion of the Brownian particle in the x direction can be investigated by the one-dimensional Langevin equation:

$$\dot{x} = v,$$

$$M\dot{v} = -\gamma(x)v - U'(x) + F + \sqrt{2\gamma(x)T(x)}\xi(t), \qquad (3)$$

where x and v are the position and velocity of the Brownian particle and $\xi(t)$ is a standard Gaussian white noise:

$$\langle\xi(t)\rangle = 0, \quad \langle\xi(t)\xi(s)\rangle = \delta(t-s). \qquad (4)$$

Here, and later on, an overdot refers to a derivative taken with respect to time and a prime means a derivative taken with respect to space. The position-dependent friction coefficient $\gamma(x)$ is assumed to be periodic and piecewise constant in the same way as temperature:

$$\gamma(x) = \begin{cases} \gamma_1 & \text{for } 0 < x \leq \frac{L}{2}, \\ \gamma_2 & \text{for } \frac{L}{2} < x \leq L. \end{cases} \qquad (5)$$

It has been shown that the Langevin equation (3) correctly predicts the behavior of Brownian particles. However, due to its mathematical difficulty, a further approximation is often used. When the relaxation time $\tau = M/\gamma$ is much smaller than a mechanical time scale $t_0 = \sqrt{ML^2/U_0}$, the inertial term in the Langevin equation (3) is usually neglected. Setting $M=0$ in Eq. (3), we obtain a popular overdamped Langevin equation,

$$\gamma(x)\dot{x} = -U'(x) + F + \sqrt{2\gamma(x)T(x)}\xi(t). \qquad (6)$$

While this equation is widely used in many different subject areas, we must be careful with $M=0$ since both τ and t_0 are zero at the same time. Strictly speaking, the overdamped condition $\tau \ll t_0$ should be satisfied only in the sense of the limit $M \to 0$.

A further complication arises when the temperature or friction coefficient depends on the position. Simple omission of the inertial term does not lead to the correct overdamped Langevin equation. One can also study stochastic processes in the overdamped limit by the equivalent Fokker-Planck equation. There is, however, no universal Fokker-Planck equation that describes a system with nonuniform temperature. Van Kampen [24] found that the particular form of the Fokker-Planck equation depends on the details of each system. For our model (overdamped Brownian particle subject to inhomogeneous temperature) the appropriate Fokker-Plank equation is given by

$$\frac{\partial P(x,t)}{\partial t} = \frac{\partial}{\partial x}\left[\frac{1}{\gamma(x)}\left([U'(x)-F]+\frac{\partial}{\partial x}T(x)\right)P(x,t)\right]. \quad (7)$$

When Eq. (7) is solved for the piecewise-constant temperature (2), the proper boundary conditions are $T_1P(\delta)=T_2P(L-\delta)$ and $T_1P(L/2-\delta)=T_2P(L/2+\delta)$, where δ is infinitesimally small [25].

Corresponding to the Fokker-Planck equation (7), the correct form of the overdamped Langevin equation, in the Stratonovich interpretation, is

$$\gamma(x)\dot{x} = -U'(x) + F + \sqrt{2T(x)\gamma(x)}\xi(t) - \frac{1}{2\gamma(x)}\frac{d}{dx}[T(x)\gamma(x)] \qquad (8)$$

as derived in [26,27]. In this paper, we shall call Eq. (8) the *overdamped* Langevin equation and refer to Eq. (3) as the *inertial* Langevin equation.

As an indicator of overdamping, we introduce a dimensionless frictional coefficient

$$\hat{\gamma} = \frac{\gamma t_0}{M} = \frac{\gamma L}{\sqrt{MU_0}}. \qquad (9)$$

When $\hat{\gamma} \gg 1$, the system is in the overdamped regime.

C. Stochastic energetics

We investigate the thermodynamic behavior of the BL system using stochastic energetics introduced by Sekimoto [1–3]. Heat flux from the gas particles in the ith cell to the Brownian particles is defined by

$$\dot{Q}_i = \langle[-\gamma_i\dot{x} + \sqrt{2\gamma_iT_i}\xi(t)]\dot{x}\rangle_i, \qquad (10)$$

where $\langle\cdots\rangle_i$ indicates the ensemble average taken while the Brownian particles are located in the ith cell. Using the inertial Langevin equation (3), Eq. (10) can be evaluated in three terms:

$$\dot{Q}_i = \frac{M}{2}\frac{d}{dt}\langle\dot{x}^2\rangle_i + \langle U'(x)\dot{x}\rangle_i - F\langle\dot{x}\rangle_i = \dot{Q}_i^{\text{KE}} + \dot{Q}_i^{\text{PE}} + \dot{Q}_i^{\text{J}}, \qquad (11)$$

where the first two terms on the right-hand side (RHS) are the kinetic energy and potential energy contribution to the heat flux, respectively, and the last term is the Joule heat.

Work done on a Brownian particle by the external force in each cell is given by

$$\dot{W}_i = F\langle\dot{x}\rangle_i. \qquad (12)$$

In the steady state, the net energy flux to the Brownian particles must be zero, and thus the energy gained by the Brownian particles in cell 1 must be canceled by the energy loss in cell 2. Therefore, heat flux from cell 1 to cell 2 via the Brownian particles is defined as

$$\dot{Q}_{1\to 2} = \dot{Q}_1 + \dot{W}_1 = \dot{Q}_1^{\text{KE}} + \dot{Q}_1^{\text{PE}}. \qquad (13)$$

D. Molecular dynamics simulation

In order to check the validity of the Langevin approach, we performed intensive molecular dynamics simulation. In our MD simulation the heat bath consists of two-dimensional hard disks of mass m and diameter σ. The Brownian particle is of mass M and diameter σ_B. Inclusion of external forces significantly reduces the numerical advantage of hard disk MD simulation. However our algorithm (see Appendix A) is fast enough to realize a sufficient number of trajectories for ensemble averaging.

In order to compare the results of Langevin approaches with those of MD simulation, we need to find the corresponding frictional coefficient. We use an analytical expression obtained for an ideal gas [28],

$$\gamma = \sigma_B \rho \sqrt{2\pi m T}, \qquad (14)$$

where ρ is the density of the gas. Note that this ideal γ does not depend on M. Alternately, we could use γ measured in the MD simulation. In fact, we can get a better agreement between the MD simulation and Langevin approaches if the measured values are used. However, the measured values depend on M, hindering the real mass dependency of the Langevin equation. Therfore, we use the theoretical frictional coefficient (14) in the Langevin equations (3) and (8).

In all our MD simulations we use $N=1000$ gas particles ($m=1$, $\sigma=1$) in each cell, with the size of each cell being 250×400, so that the density $\rho=0.01$. The spatial period of the piecewise-linear potential is $L=500$ and the barrier height $U_0=1.0$. As the temperature of the reservoirs changes during the course of the simulation there is no well-defined stationary state. However, all our simulations were carried out using a sufficiently large number of gas particles so that the system remains in a quasi-steady-state for a sufficiently long period of time, enabling us to measure the various physical quantities properly.

III. HEURISTIC DISCUSSION WITH THE OVERDAMPED MODEL

In this section we first review the known properties of the BL motor and its reciprocal process the BL refrigerator, in the overdamped limit. When the temperatures of the cells are different $(T_1 > T_2)$, the Brownian particles in the high-temperature cell can reach a higher-potential-energy region than those in the low-temperature cell. Hence, the Brownian particles tend to move from the hot cell to the cold cell over the potential barrier. At the other cell boundary, the potential is minimum and both cold and hot Brownian particles can easily cross to the other side. Therfore, the Brownian particles flow in the positive-x direction on average even in the absence of external force $(F=0)$. When an external load is applied $(F<0)$, the Brownian particles can do work against it as a motor.

Asymmetry in the spatial distribution of the Brownian particles due to the temperature difference is the main driving of this motor. The overdamped Langevin equation (8) or Fokker-Planck equation (7) provides an analytical expression for the spatial distribution, from which we obtain the average velocity of the motor (see Appendix B):

$$\langle v \rangle = \frac{2 \sinh(\phi_1 + \phi_2)}{(\gamma_1/\phi_1 - \gamma_2/\phi_2)(1/f_1 - 1/f_2)\sinh\phi_1 \sinh\phi_2 - (\gamma_1/f_1 + \gamma_2/f_2)\sinh(\phi_1 + \phi_2)}, \qquad (15)$$

where $f_{1,2}=-F \pm 2U_0/L$ and $\phi_i=-f_i L/(4T_i)$. In the absence of external force $(F=0)$, Eq. (15) is always positive for $T_1 > T_2$ and hence the Brownian particles move in the positive direction as expected. In fact, the particle distribution and velocity in the overdamped regime agree reasonably well with the results obtained from numerical simulation of the inertial Langevin equation and molecular dynamics simulation (see Figs. 2 and 3), suggesting the validity of the overdamped Langevin equation.

Now, we consider the thermodynamic efficiency of the BL motor. Based on the successful prediction of particle distribution and velocity it is natural to use the overdamped Langevin approach for other quantities such as efficiency. Applying the overdamped Langevin equation (8) to the definition of heat (10), the heat flux from the heat bath to the Brownian particles in cell 1 is given by

$$\dot{Q}_1 = \left\langle \frac{1}{2\gamma(x)}\frac{d}{dx}[\gamma(x)T(x)]\dot{x} \right\rangle_1 + \langle U'(x)\dot{x}\rangle_1 - F\langle\dot{x}\rangle_1. \qquad (16)$$

Comparing this equation with Eq. (11), the first term in the RHS of Eq. (16) corresponds to the kinetic energy contribution $\dot{Q}_i^{\mathrm{KE}}$. However, due to the periodic boundary condition and Eq. (14), this kinetic energy contribution vanishes [20]

and we obtain $\dot{Q}_1=(2U_0/L-F)\langle\dot{x}\rangle_1$. Hence, we find the efficiency of the motor

$$\eta = \frac{-\dot{W}}{\dot{Q}_1} = \frac{-2F}{2U_0/L - F}, \qquad (17)$$

where $\dot{W}=F\langle v\rangle$. When the motor is in a stalled state $(\phi_1 + \phi_2=0)$, we can show that the efficiency reaches the Carnot efficiency $\eta_C=1-T_2/T_1$.

This result is puzzling since at the moment a Brownian particle enters the cold bath it is carrying $T_1/2$ of kinetic energy. When it is thermalized with the cold bath, $Q_{1\to2}^{\mathrm{KE}} \propto (T_1-T_2)/2$ of heat dissipates into the cold bath. This heat dissipation takes place whenever the Brownian particle crosses a temperature boundary and it is irreversible. Due to diffusion, the crossing occurs even when the average velocity vanishes, and this irreversible heat transfer due to thermal fluctuation of Brownian particles never ceases as long as there is a steep temperature gradient. Derényi and Astumian [18] and Hondou and Sekimoto [19] have pointed out that the kinetic energy contribution is the dominant channel of heat transfer between two cells and thus the efficiency of the BL motor cannot reach the Carnot efficiency. This situation is similar to the case of the FS motor [1,8].

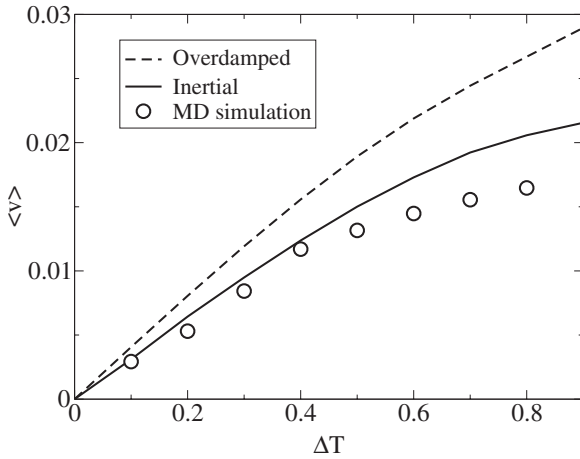An interesting question is why the overdamped Langevin

FIG. 2. Mean velocity as a function of the temperature difference $\Delta T = T_1 - T_2$ between the two cells. The average temperature of the whole system is fixed to $T_{av} = (T_1 + T_2)/2 = 0.5$. Solid and dashed lines correspond to data obtained from the inertial Langevin equation (3) and the overdamped Langevin equation (8), respectively, while circles correspond to MD simulation. The parameter values are $M/m = 4.0$, $\sigma_B = 4.0$, and $F = 0$. The dimensionless frictional coefficients vary from $\hat{\gamma}_1 = \hat{\gamma}_2 = 17.7$ at $\Delta T = 0$ to $\hat{\gamma}_1 = 24.4$ and $\hat{\gamma}_2 = 5.6$ at $\Delta T = 0.9$. As $\hat{\gamma}_2$ becomes less overdamped with the increase of ΔT, the overdamped model deviates from the inertial Langevin equation.

approach failed for the BL motor whereas it worked fine for the FS motor. Derényi and Astumian [18] and also Hondou and Sekimoto [19] answered this question phenomenologically. Consider the thermal velocity $v_{th} = \sqrt{T/M}$. When a Brownian particle crosses the temperature boundary, it will not be immediately thermalized and there is a narrow region $\ell_{th} = v_{th}\tau = \sqrt{TM}/\gamma$ where the average kinetic energy of the Brownian particle does not coincide with the temperature of the reservoir (see lower panel of Fig. 3). In the overdamped limit ($M \to 0$), this region vanishes, justifying the use of the overdamped approach. However, the effective temperature gradient is $|T_1 - T_2|/\ell_{th} \propto M^{-1/2}$. Hence, the heat current is proportional to $M^{-1/2}$ and diverges as $M \to 0$. This singularity implies that the overdamped regime that assumes $M = 0$ is not equivalent to the overdamped limit $M \to 0$. Apparently, the FS motor does not have this problem [1]. One of our objectives is to verify this singular behavior by numerical simulations.

Next, we turn to the BL refrigerator. We assume $T_1 = T_2 = T$ and apply a weak external force $0 < F < 2U_0/L$ to the Brownian particle. Due to the external force, the Brownian particle drifts in the direction of F and its average velocity in the overdamped limit can be obtained from Eq. (15). Unlike the motor case, the temperature is uniform throughout the system and thus the kinetic energy does not contribute significantly to the heat exchange between the cells. Again using the overdamped model, the heat flux absorbed by the Brownian particle from the ith reservoir is obtained from Eq. (16) as
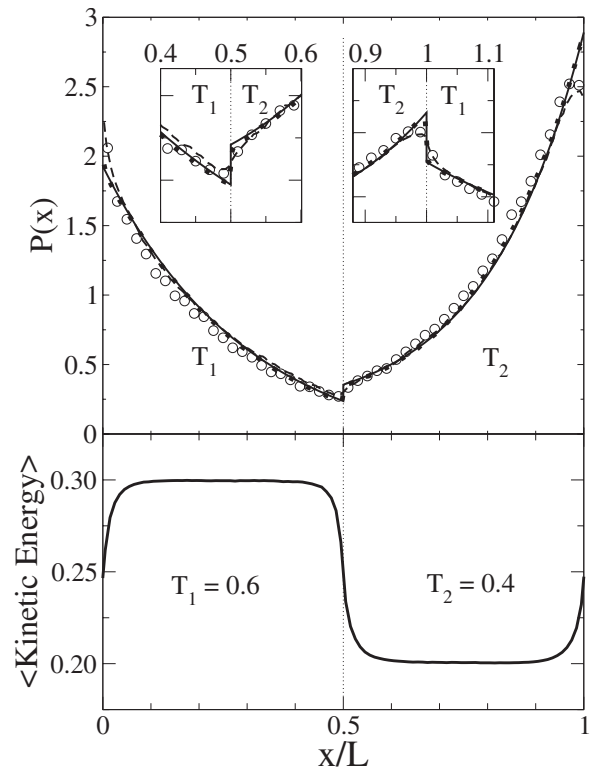
FIG. 3. Upper panel: Steady state spatial distribution $P(x)$ of Brownian particles as obtained from the Fokker-Planck equation (7) (solid line), overdamped Langevin equation (8) (dotted line, mostly hidden under the solid lines), inertial Langevin equation (3) (dashed line), and MD simulation (circles). The parameter values are $M/m = 5.0$, $\sigma_B = 6.0$, $T_1 = 0.6$, $T_2 = 0.4$, and $F = 0$. $\hat{\gamma}_1 = 26.0$ and $\hat{\gamma}_2 = 21.3$ correspond to the overdamped regime. The two insets show the details of $P(x)$ near the temperature boundaries at $x/L = 0.5$ and 1.0. Lower panel: The locally averaged kinetic energy of the Brownian particle along the x axis, obtained from the inertial Langevin equation (3).

$$\dot{Q}_1 = + \frac{2U_0}{L}\langle \dot{x} \rangle_1 - F\langle \dot{x} \rangle_1, \quad \dot{Q}_2 = - \frac{2U_0}{L}\langle \dot{x} \rangle_2 - F\langle \dot{x} \rangle_2,$$

(18)

where the first term is the potential energy contribution $\dot{Q}_i^{PE}$ and the second term the Joule heat $\dot{Q}_i^{J}$. Since $\dot{Q}_i^{PE} \propto F$ and $\dot{Q}_i^{J} \propto F^2$ we can have positive $\dot{Q}_1$ for sufficiently small F, indicating that cell 1 is refrigerated. Since there is no singular behavior due to temperature change, the overdamped model may be good enough. However, as soon as refrigeration induces a temperature difference between the cells, the heat transfer due to the kinetic energy reduces the power of refrigeration. Our second objective is to investigate whether the overdamped model is sufficient and if the refrigeration can be sustained against the heat leak due to the kinetic energy.

The BL motor and refrigerator are a result of a cross effect between the external force F and the temperature difference ΔT. Assuming they are small, we can make a connection between the motor and refrigerator using linear irreversible thermodynamics expressed by

$$\langle v \rangle = L_{11}\frac{F}{T} + L_{12}\frac{\Delta T}{T^2},$$

$$\dot{Q}_{1\to 2} = L_{21}\frac{F}{T} + L_{22}\frac{\Delta T}{T^2}, \qquad (19)$$

where the transport coefficients are defined as

$$L_{11} = T\frac{\partial\langle v\rangle}{\partial F}, \quad L_{12} = T^2\frac{\partial\langle v\rangle}{\partial\Delta T},$$

$$L_{21} = T\frac{\partial\dot{Q}_{1\to 2}}{\partial F}, \quad L_{22} = T^2\frac{\partial\dot{Q}_{1\to 2}}{\partial\Delta T}. \qquad (20)$$

Here, the partial derivatives are evaluated at $\Delta T = 0$ and $F = 0$. In the overdamped case we can obtain all Onsager coefficients from Eqs. (13), (15), and (16) as

$$L_{11} = \frac{U_0^2}{T}\xi, \quad L_{22} = \frac{U_0^4}{TL^2}\xi, \quad L_{12} = L_{21} = \frac{U_0^3}{TL}\xi, \qquad (21)$$

where $\xi = [4\gamma \sinh^2(U_0/2T)]^{-1}$. These coefficients support the Onsager symmetry $L_{12} = L_{21}$. Moreover, Eq. (21) indicates $L_{11}L_{22} - L_{12}L_{21} = 0$, implying no entropy production [29], and thus the motor operates at the Carnot efficiency. Hence the overdamped model again erroneously predicts the highest possible efficiency. The singular behavior of $\dot{Q}_{1\to 2}$ at $M = 0$ casts some doubt on the Onsager symmetry since the two limits $M \to 0$ and $\Delta T \to 0$ do not commute. Our third objective is to numerically investigate the validity of linear irreversible theory and the Onsager symmetry at the overdamped limit.

IV. RESULTS

A. Motor

First we show in Fig. 3 that the numerical solution of the overdamped Langevin equation (8) agrees perfectly with the solution of the corresponding Fokker-Planck equation (7), confirming that the extra term in Eq. (8) is necessary. Furthermore, the results of overdamped Langevin equation are in good agreement with the numerical results from the inertial Langevin equation (3) and molecular dynamics simulation, except for narrow regions at the temperature boundaries (see the insets in Fig. 3). Although it is in general small, this error in the overdamped regime should not be overlooked.

As we discussed in Sec. III, the overdamped Langevin method assumes that the Brownian particles are locally in equilibrium with the the thermal reservoir. Therefore, the average kinetic energy of the Brownian particles is assumed to be the same as the local temperature of the heat bath. This assumption, however, fails near the temperature boundaries, since the Brownian particles entering from one temperature region to another are not immediately thermalized with the new environment even when the mass is very small, as Fig. 3 indicates. The size of the transition region is the thermalization length ℓ_{th}. In the overdamped limit ($M \to 0$), the transition region indeed vanishes but only slowly as $\sqrt{M}$.
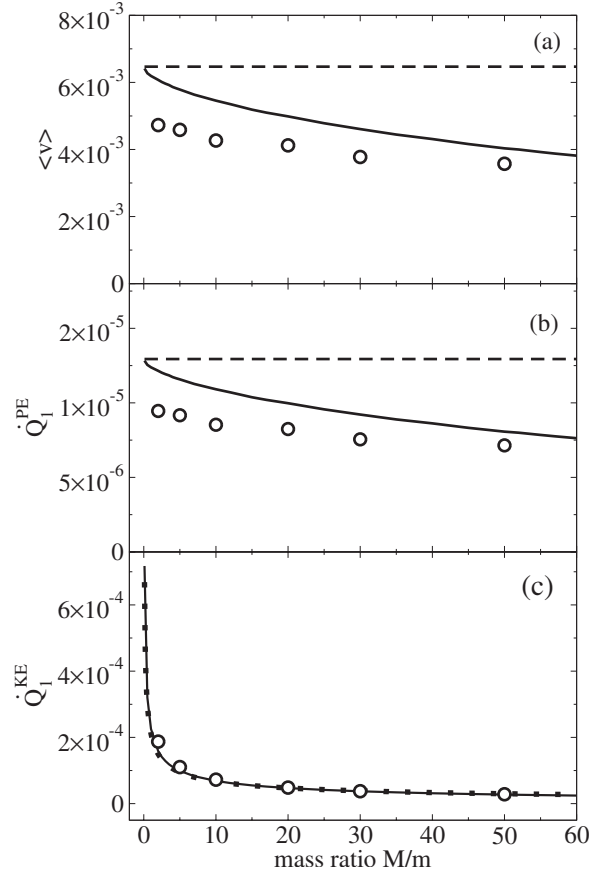

FIG. 4. Mean velocity (a), heat flux due to potential energy (b), and heat flux due to kinetic energy (c) as a function of the mass ratio M/m. Circles, dashed lines, and solid lines correspond to MD simulation, overdamped model, and inertial Langevin equation, respectively. The parameter values are $T_1 = 0.6$ and $T_2 = 0.4$, $\sigma_B = 5.0$, and $F = 0.0$. As the mass ratio changes from $M/m = 0.1$ to 60, $\hat{\gamma}_1$ varies from 48.5 to 6.3, and $\hat{\gamma}_2$ varies from 39.6 to 5.1. In (c) the dotted line indicates $0.000\,215(M/m)^{-1/2}$, an empirical fit to the result of the inertial Langevin equation.

It turns out that such a subtle error in the overdamped Langevin method does not lead to large errors in certain quantities obtained from it. Figure 2 shows that the overdamped Langevin equation predicts the average velocity as well as does the inertial Langevin equation. Due to this success we feel safe in using the overdamped approach to compute other quantities. However, the calculation of the heat is a different story. As we discussed in the previous section, the overdamped approach predicts that the heat transfer between the cells is only from potential energy contribution. However, Hondou and Sekimoto [19] pointed out that the narrow transition region plays a dominant role in heat transfer and the overdamped Langevin equation fails in the investigation of heat calculations. The inertial Langevin approach concludes that the kinetic energy contribution is actually dominant.

Using scaling arguments, Derényi and Astumian [18] and Hondou and Sekimoto [19] predicted that the kinetic energy contribution diverges as $M^{-1/2}$ at $M = 0$. Figure 4 clearly shows such a singularity, in good agreement with their theory, and confirms $\dot{Q}_1^{KE} \gg \dot{Q}_1^{PE}$. We also find from Fig. 4
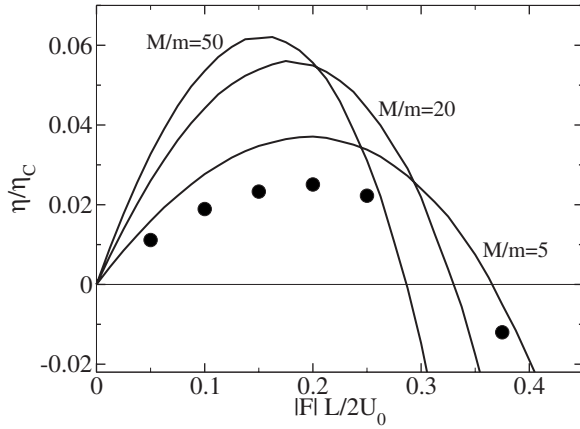
FIG. 5. Efficiency of the motor vs the magnitude of the external load, for mass ratios $M/m=5.0$, 20.0, and 50.0. Solid lines correspond to numerical solution of the inertial Langevin equation and solid circles represent MD simulation (for $M/m=5.0$ only). Other parameter values are $T_1=0.7$, $T_2=0.3$, and $\sigma_B=5.0$. The dimensionless friction coefficients are $\hat{\gamma}_1=23.4$, $\hat{\gamma}_2=15.3$ for $M/m=5.0$; $\hat{\gamma}_1=11.7$, $\hat{\gamma}_2=7.7$ for $M/m=20.0$; and $\hat{\gamma}_1=7.4$, $\hat{\gamma}_2=4.9$ for $M/m=50.0$.

that the result obtained from the inertial Langevin equation approaches the MD simulation result as the mass ratio M/m increases. Even for small M/m, the inertial Langevin equation predicts the correct order of magnitude of the motor velocity and the heat flows, though, in general, the Langevin approach is not applicable in such a case. The motor velocity and heat flow via potential energy predicted by the overdamped model, deviate from the inertial Langevin equation and MD simulation result as the mass ratio increases because the inertial effect becomes too large to be ignored. The good agreement between the inertial Langevin equation and the molecular dynamics simulation shows that Hondou and Sekimoto's definition of stochastic energetics predicts the heat correctly even when the temperature is spatially inhomogeneous.

In Fig. 5, we plot the efficiency of the motor normalized by the Carnot efficiency η_C, as a function of the external load F normalized by the magnitude of the force exerted by the periodic potential energy. In contradiction to the overdamped model, the efficiency is far below the Carnot limit. While this result was phenomenologically argued for in [18,19], here we confirmed with molecular dynamics simulation and numerical solution of the inertial Langevin equation that the kinetic energy contribution greatly reduces the efficiency. Even when the motor is operated at the quasistatic limit with a stall force, the irreversible heat transfer via kinetic energy persists and thus the Carnot limit is unattainable. Furthermore, the divergence of $\dot{Q}_1^{KE}$ at $M=0$ diminishes the efficiency of the motor to zero, in the overdamped limit.

B. Refrigerator

In the refrigerator mode, two cells initially have the same temperature and the Brownian particles are driven by an external force F. In Fig. 6, MD simulation illustrates the cool-
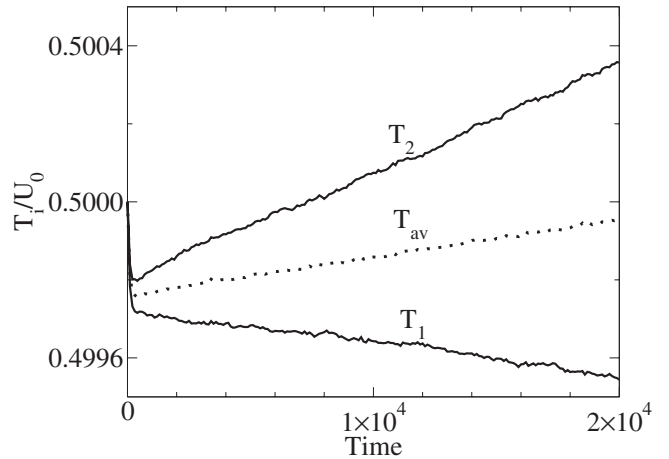

FIG. 6. Temperatures of cells 1 and 2 and the average temperature $T_{av}=(T_1+T_2)/2$ as a function of time obtained from MD simulation. Initial temperatures of cells 1 and 2 are $T_1=T_2=T=0.5$ and an external force $FL/(2U_0)=0.5$ is applied to the Brownian particle in the positive direction. The other parameter values are $M/m=20$ and $\sigma_B=8.0$, leading to a dimensionless frictional coefficient $\hat{\gamma}_1=\hat{\gamma}_2=15.9$ (overdamped regime). Temperature drops at the beginning because the Brownian particles are initially at rest.

ing of cell 1 at the expense of the heating of cell 2. Note, however, that the average temperature T_{av} increases with time as Joule heat is dissipated in both the cells. In the Langevin approach, we cannot see such temperature changes since the temperature needs to be kept constant. However, it allows us to investigate heat transfer between the cells. Figure 7 shows the components of heat from cell 1 to the Brownian particles as a function of F. The potential energy contribution increases linearly with F whereas Joule heat decreases ($\dot{Q}_1^J<0$) as F^2 [see Eq. (18)]. For sufficiently small
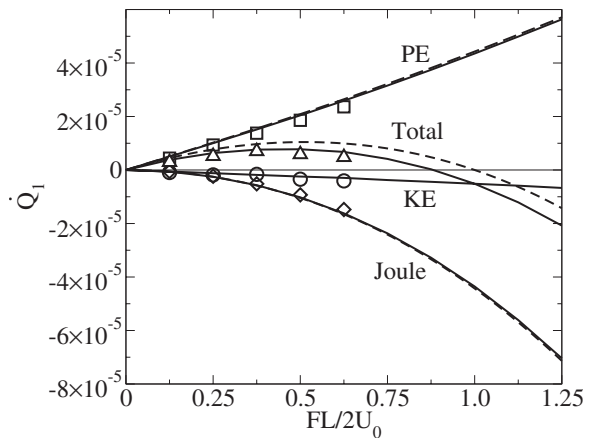

FIG. 7. Various components of $\dot{Q}_1$ of the refrigerator as a function of the external force. From top to bottom the heat flows are the potential energy contribution ($\dot{Q}_1^{PE}$), total heat ($\dot{Q}_1$), kinetic energy contribution ($\dot{Q}_1^{KE}$), and Joule heat ($\dot{Q}_1^J$), respectively. Symbols represent corresponding MD simulation, dashed lines the overdamped Langevin equation, and solid lines the inertial Langevin equation. The parameter values are $M/m=20.0$, $\sigma_B=8.0$, and $T_1=T_2=0.5$ so that $\hat{\gamma}_1=\hat{\gamma}_2=15.9$ (overdamped).
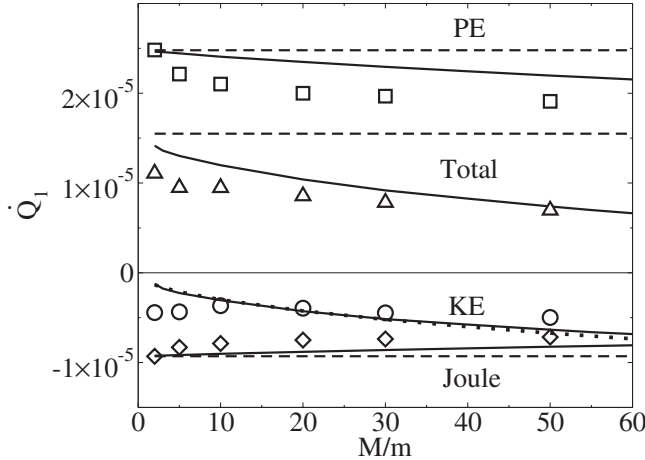
FIG. 8. Various components of $\dot{Q}_1$ of the refrigerator as a function of the mass. From top to bottom the heat flows are the potential energy contribution ($\dot{Q}_1^{PE}$), total heat ($\dot{Q}_1$), kinetic energy contribution ($\dot{Q}_1^{KE}$), and Joule heat ($\dot{Q}_1^J$), respectively. Symbols represent MD simulation, dashed lines the overdamped Langevin equation, and solid lines the inertial Langevin equation. The dotted line represents a fit ($\propto \sqrt{M/m}$) to the kinetic energy contribution according to Eq. (22). The parameter values are $\sigma_B = 5.0$, $T_1 = T_2 = 0.5$, and $FL/(2U_0) = 0.375$. The dimensionless friction coefficients ($\hat{\gamma}_1 = \hat{\gamma}_2$) vary from 31.3 at $M/m = 2.0$ (overdamped) to 5.7 at $M/m = 60.0$ (weakly damped).

F, the potential energy contribution wins, and hence the Brownian particles extract heat from cell 1 and dump it in cell 2. There is an optimal F at which the cooling effect is maximum. The agreement between the overdamped and inertial Langevin equations and with the molecular dynamics simulation is good for $\dot{Q}_1^{PE}$ and $\dot{Q}_1^J$.

Since the temperature is uniform, we do not expect significant kinetic energy contribution. However, in Fig. 7, we found that there is a small kinetic energy contribution which is absent in the overdamped approach. In the overdamped regime we assume that the change in potential energy immediately dissipates into the reservoir. However, with a finite mass, the potential energy is first converted to kinetic energy which dissipates at a later time. For example, when a Brownian particle slides down the potential slope near a cell boundary, the potential energy change is transported to the next cell as kinetic energy where it is dissipated as heat. The amount of "unthermalized" kinetic energy the Brownian particles acquire from the potential energy is approximately

$$\dot{Q}_1^{KE} \approx -U'(x)\ell_{th}\frac{\langle \dot{x}\rangle}{L} = -\frac{2U_0\langle \dot{x}\rangle}{\gamma L^2}\sqrt{MT}, \quad (22)$$

which is linear with F through $\langle \dot{x}\rangle$ in agreement with the result of the inertial Langevin equation (see Fig. 7). Both this kinetic energy (KE) contribution and the potential energy (PE) contribution are in proportion to F, yet the magnitude of $\dot{Q}_1^{KE}$ is negligibly small compared to that of $\dot{Q}_1^{PE}$ at the overdamped limit. Therefore, the refrigeration is still possible. Figure 8 shows that the PE contribution approaches the overdamped model as $M \rightarrow 0$. The KE contribution approaches
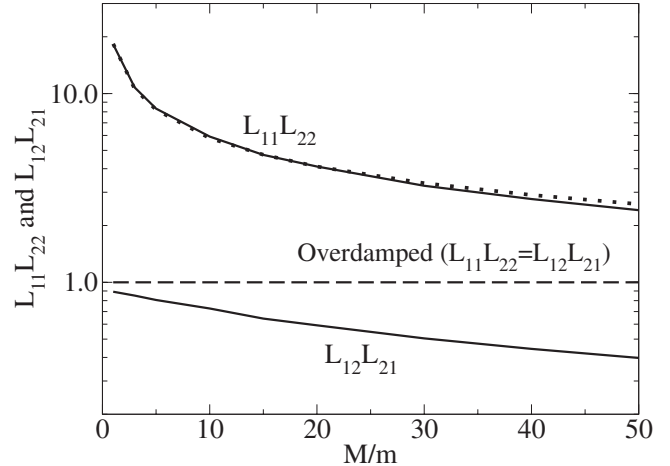

FIG. 9. Product of the Onsager coefficients $L_{11}L_{22}$ and $L_{12}L_{21}$ as a function of M/m obtained from the inertial Langevin equation. The dotted line is the phenomenological fit $18.4(M/m)^{-1/2}$ to the product $L_{11}L_{22}$. The dashed line represents the Onsager coefficients obtained from overdamped results. All data have been normalized with respect to the overdamped value. We use a logarithmic scale for the y axis. The parameters for obtaining L_{12} and L_{22} were $\Delta T = 0.025$ and $F = 0$, while L_{11} and L_{21} were obtained at $\Delta T = 0$ and $FL/(2U_0) = 0.025$, where $T_1 = (1/2)(1+\Delta T)$, $T_2 = (1/2)(1-\Delta T)$, and $\sigma_B = 5.0$.

zero as $(M/m)^{1/2}$, in good agreement with the phenomenological prediction (22). Figures 7 and 8 both show that the overdamped model is in good agreement with the inertial Langevin equation as well as the MD simulation in predicting the velocity and heat flows.

The overdamped Langevin equation seems to work well for the refrigerator. However, the cooling effect creates a temperature difference between the two reservoirs and the overdamped approach again fails. In turn, the temperature difference induces a thermodynamic force opposing the external force F, through the Brownian motor mechanism. As the temperature difference increases, the motor and refrigerator effects eventually cancel each other, so that the average velocity of the Brownian particle becomes zero and the cooling ceases.

C. Onsager symmetry

As discussed in Sec. III, we need to evaluate the transport coefficients (20) with a certain care. Since the heat transfer diverges when the limit $M \rightarrow 0$ is taken before $\Delta T \rightarrow 0$, we first evaluate the coefficients at finite mass numerically from response curves like Figs. 2 and 7. Then we reduce the mass toward $M = 0$. Figure 9 shows that, as M decreases, the product of off-diagonal coefficients approaches the result of the overdamped Langevin equation obtained from Eq. (21). However, the product of diagonal coefficients diverges as $(M/m)^{-1/2}$, reflecting the divergence of $\dot{Q}^{KE}$. As expected, the off-diagonal coefficients do not suffer from the singular inertial effect. Furthermore, Fig. 9 shows that $L_{11}L_{22} \gg L_{12}L_{21}$ for all values of M/m, indicating large entropy production, consistent with the very low efficiency. Finally, Fig.
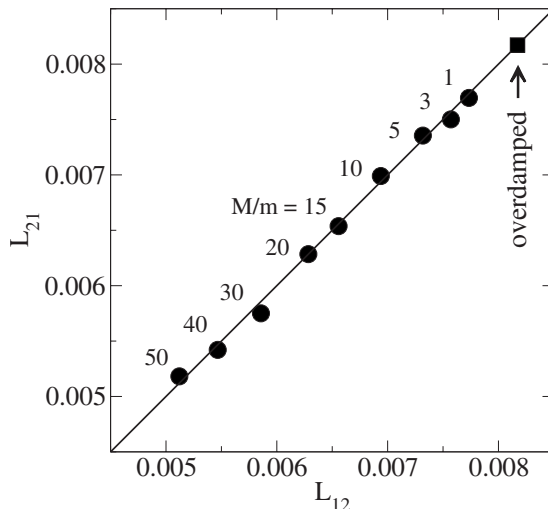
FIG. 10. Onsager reciprocity coefficient L_{21} vs L_{12} for various M/m. The parameter values are the same as in Fig. 9. The solid circles represent data obtained from the inertial Langevin equation. The value obtained from the overdamped model is shown with a solid square.

10 numerically verifies the Onsager symmetry for all masses within the accuracy of simulation and shows that the overdamped model (21) predicts the correct overdamped limit.

V. DISCUSSION

In this paper, we investigated the thermodynamic properties of the BL motor and refrigerator using Langevin equations and molecular dynamics simulation. For mechanical properties such as the velocity of the Brownian particles, we observed reasonable agreement between results of the overdamped Langevin equation and molecular dynamics simulation. However, the overdamped Langevin equation failed to predict thermodynamic properties such as the heat transfer. On the other hand, we found good agreement between the inertial Langevin equation and molecular dynamics simulation even in the overdamped regime. Therefore, we conclude that the inertial mass plays a significant role even in the overdamped limit. The main effect of the inertial mass is the kinetic energy contribution to the heat transfer. We confirmed that the kinetic energy contribution is dominant when two cells have different temperatures, and verified the previous phenomenological prediction that the irreversible kinetic energy contribution diverges as $M^{-1/2}$ at the overdamped limit.

Recently, Van den Broeck [30] investigated the efficiency of Brownian motors using linear irreversible thermodynamics and concluded that, in principle, Carnot efficiency can be attained. He argues that, when the load F is small, the temperature difference ΔT drives the motor in the forward direction and at the same time the motor transfers heat from the high- to the low-temperature reservoir. As the load exceeds the stall force, the motor moves backward, transferring heat against the temperature gradient as a heat pump. In an ideal system, the directions of velocity and heat are reversed at the same magnitude of the external force. Hence, the thermody-

namic fluxes $\langle v \rangle$ and $\dot{Q}_{1 \rightarrow 2}$ simultaneously vanish despite F and ΔT not being zero. This can happen only when $L_{11}L_{22} - L_{12}L_{21} = 0$ and thus Carnot efficiency is achieved.

In our case, the direction of $\dot{Q}^{PE}$ coincides with the direction of $\langle v \rangle$, and both $\dot{Q}^{PE}$ and $\langle v \rangle$ vanish at the stall force. However, $\dot{Q}^{KE}$ flows from the hot to the cold reservoir regardless of the direction of $\langle v \rangle$. Therefore, $\dot{Q}^{KE}$ does not necessarily vanish. In fact, it never vanishes and the Carnot efficiency cannot be achieved in the BL system. The efficiency of the BL motor is significantly reduced by the kinetic energy contribution and vanishes at the overdamped limit.

Dérenyi and Astumian [18] have argued that, if we could prevent the recrossing of the Brownian particle over the temperature boundary, such irreversible heat transfer could be arbitrarily reduced and thus the efficiency would be greatly improved. They proposed to place a gate at each temperature boundary which prevents Brownian particles from crossing the boundary back and forth multiple times during a short period of time. If such a gate were possible, the motor could reach Carnot efficiency. However, it is not clear at present how to construct such a gate without reducing the particle velocity. Based on naive considerations, one might expect significant reduction of the kinetic energy contribution by optimizing the potential profile and the location of the temperature boundary. Unfortunately, the reduction of heat transfer always results in the reduction of the motor velocity as well and the gain in the efficiency is very limited [31].

Recently, Humphrey et al. [32] proposed a quantum Brownian heat engine which achieves Carnot efficiency. In this model, reversible particle exchange between two cells is achieved by filtering the energy of the particle, without violating the second law. The filter allows only particles having a certain energy, for which the Fermi-Dirac distributions in the two cells coincide, to pass through. This ensures that the particle flow does not alter the thermal distribution in either cell so that there is no kinetic energy contribution. Hence, the heat engine attains Carnot efficiency in the quasistatic limit. Whether a similar heat engine can be devised in the classical regime is not clear.

APPENDIX A: HARD DISK MOLECULAR DYNAMICS SIMULATION

Our hard disk molecular dynamics simulation is based on a usual event-driven algorithm [33]. In the case of collision between two gas particles the collision time can be obtained analytically as given in [33]. However, since the Brownian particle is subject to forces due to the piecewise-linear potential $U(x)$ and the external load F, the calculation of collision time between a Brownian particle and a gas particle is not straightforward. Suppose that we know the relative position **r** and relative velocity **v** of a Brownian particle with

respect to a gas particle at time t_0. We want to find the time $t = t_0 + \epsilon$, at which they collide. The distance between two particles at the moment of impact is $d = (\sigma + \sigma_B)/2$ and hence

$$\left| \mathbf{r} + \mathbf{v}\epsilon + \frac{1}{2}\mathbf{a}\epsilon^2 \right| = d, \quad \text{(A1)}$$

where $\mathbf{a}$ is the constant acceleration of the Brownian particle. (Note that the gas particle has no acceleration.) To find ϵ, we rewrite Eq. (A1) as a quartic equation for $a \neq 0$,

$$\epsilon^4 + A\epsilon^3 + B\epsilon^2 + C\epsilon + D = 0, \quad \text{(A2)}$$

where $A = 4\mathbf{v}\cdot\mathbf{a}/a^2$, $B = 4(\mathbf{a}\cdot\mathbf{r} + v^2)/a^2$, $C = 8\mathbf{r}\cdot\mathbf{v}/a^2$, and $E = 4(r^2 - d^2)/a^2$. Using a standard method [34], we find four solutions

$$\epsilon = -\frac{A}{4} + \frac{1}{2}(F \pm \sqrt{G + H}), \quad \epsilon = -\frac{A}{4} - \frac{1}{2}(F \pm \sqrt{G - H}), \quad \text{(A3)}$$

where

$$F = \pm \sqrt{\frac{A^2}{4} - B + x}, \quad \text{(A4)}$$

$$G = \frac{3}{4}A^2 - F^2 - 2B, \quad \text{(A5)}$$

$$H = \begin{cases} \dfrac{4AB - 8C - A^3}{4F} & \text{if } F \neq 0, \\ 2\sqrt{x^2 - 4D} & \text{if } F = 0, \end{cases} \quad \text{(A6)}$$

and x is a real solution of an auxiliary equation,

$$x^3 - Bx^2 + (AC - 4D)x + 4BD - C^2 - A^2D = 0. \quad \text{(A7)}$$

The analytical solutions to the cubic equation (A7) are given in [35].

The correct collision time corresponds to the smallest positive real root of Eq. (A3), if it exists. Despite having analytical solutions, this algorithm occasionally fails, particularly when the acceleration a is significantly small, because some of the coefficients become extremely large, causing bit-off errors. To overcome this difficulty, we improve the accuracy of the roots by iterating the Newton-Raphson

[35] steps a few times starting from the analytical solution to Eq. (A7). We found that the present algorithm is faster than a direct solution of the quartic equation (A2) by the Newton-Raphson method.

APPENDIX B: ANALYTICAL EXPRESSIONS IN THE OVERDAMPED CASE

We derive analytical expressions for the steady state density $P(x)$ and current $J(x)$. The Fokker-Planck equation for steady states is simply $dJ(x)/dx = 0$, where the particle current is defined by

$$\gamma(x)J(x) = -[U'(x) - F]P(x) - \frac{d}{dx}[T(x)P(x)]. \quad \text{(B1)}$$

In our model, the Fokker-Planck equation for the ith cell is given by

$$P_i''(x) + \frac{f_i}{T_i}P_i'(x) = 0 \quad (i = 1,2), \quad \text{(B2)}$$

where the net force is defined as $f_{1,2} = -F \pm 2U_0/L$. We consider only weak external forces $|F| < F_c = 2U_0/L$ so that it does not destroy the potential barrier and hence we assume $f_i \neq 0$. Thus we find the general solutions

$$P_1(x) = C_1 \exp\left(-\frac{f_1 x}{T_1}\right) + D_1, \quad \text{(B3)}$$

$$P_2(x) = C_2 \exp\left(-\frac{f_2(x - L)}{T_2}\right) + D_2, \quad \text{(B4)}$$

where C_i and D_i are the constants of integration. The corresponding currents are $J_i = -D_i f_i / \gamma_i$ $(i = 1, 2)$. Since temperature and frictional coefficient are discontinuous at the cell boundaries, the density does not have to be continuous. However, the current must be continuous $(J_1 = J_2 = J)$. From Eq. (B1), we find the magnitude of the density discontinuity as $T_1 P_1(L/2) = T_2 P_2(L/2)$ and $T_1 P_1(0) = T_2 P_2(L)$ [25]. These boundary conditions along with normalization of the density are sufficient to determine the integration constants. After obtaining an expression for J and the integration constants, we obtain a general expression for the average velocity [Eq. (15)] from the general relation $\langle v \rangle = JL$. The particle density in each cell is obtained from Eqs. (B3) and (B4).

[1] K. Sekimoto, J. Phys. Soc. Jpn. **66**, 1234 (1997).
[2] K. Sekimoto, Prog. Theor. Phys. Suppl. **130**, 17 (1998).
[3] K. Sekimoto (unpublished).
[4] P. Reimann, Phys. Rep. **361**, 57 (2002).
[5] R. P. Feynman, R. B. Leighton, and M. Sands, *The Feynman Lectures on Physics* (Addison Wesley, Reading, MA, 1966), Vol. I, Chap. 46.
[6] M. Büttiker, Z. Phys. B: Condens. Matter **68**, 161 (1987).
[7] R. Landauer, J. Stat. Phys. **53**, 233 (1988).
[8] J. M. R. Parrondo and P. Español, Am. J. Phys. **64**, 1125

(1996).
[9] T. Hondou and F. Takagi, J. Phys. Soc. Jpn. **67**, 2974 (1998).
[10] C. Van den Broeck, R. Kawai, and P. Meurs, Phys. Rev. Lett. **93**, 090601 (2004).
[11] E. Kestemont, C. Van den Broeck, and M. Malek Mansour, Europhys. Lett. **49**, 143 (2000).
[12] C. Van den Broeck, E. Kestemont, and M. Malek Mansour, Europhys. Lett. **56**, 771 (2001).
[13] C. Jarzynski and O. Mazonka, Phys. Rev. E **59**, 6448 (1999).
[14] C. Van den Broeck and R. Kawai, Phys. Rev. Lett. **96**, 210601

(2006).

[15] N. Nakagawa and T. S. Komatsu, Europhys. Lett. **75**, 22 (2006).

[16] M. Bier and R. D. Astumian, Bioelectrochem. Bioenerg. **39**, 67 (1996).

[17] Y. M. Blanter and M. Büttiker, Phys. Rev. Lett. **81**, 4040 (1998).

[18] I. Derényi and R. D. Astumian, Phys. Rev. E **59**, R6219 (1999).

[19] T. Hondou and K. Sekimoto, Phys. Rev. E **62**, 6021 (2000).

[20] M. Matsuo and S.-I. Sasa, Physica A **276**, 188 (2000).

[21] M. Asfaw and M. Bekele, Eur. Phys. J. B **38**, 457 (2004); Phys. Rev. E **72**, 056109 (2005); Physica A **384**, 346 (2007).

[22] B.-Q. Ai, H.-Z. Xie, D.-H. Wen, X.-M. Liu, and L.-G. Liu, Eur. Phys. J. B **48**, 101 (2005); B.-Q. Ai, L. Wang, and L.-G. Liu, Phys. Lett. A **352**, 286 (2006).

[23] N. G. van Kampen, J. Stat. Phys. **63**, 1019 (1991).

[24] N. G. van Kampen, IBM J. Res. Dev. **32**, 107 (1988).

[25] The boundary conditions for a system with inhomogeneous temperature are discussed in Ref. [7]. Different boundary conditions, namely, $P_1(0)=P_2(L)$ and $P_1(L/2)=P_2(L/2)$, are often used in the literature [16,21]. However, these boundary conditions are not consistent with the physical system under consideration. Indeed, the solution obtained with these boundary conditions disagrees with the results of our molecular dynamics simulation both qualitatively and quantitatively.

[26] J. M. Sancho, M. S. Miguel, and D. Duerr, J. Stat. Phys. **28**, 291 (1982).

[27] A. M. Jayannavar and M. C. Mahato, Pramana, J. Phys. **45**, 369 (1995).

[28] P. Meurs, C. Van den Broeck, and A. Garcia, Phys. Rev. E **70**, 051109 (2004).

[29] S. R. de Groot and P. Mazur, *Non-Equilibrium Thermodynamics* (Dover, New York, 1984).

[30] C. Van den Broeck, Adv. Chem. Phys. **135**, 189 (2007).

[31] R. Benjamin and R. Kawai (unpublished).

[32] T. E. Humphrey, R. Newbury, R. P. Taylor, and H. Linke, Phys. Rev. Lett. **89**, 116801 (2002).

[33] D. C. Rapaport, *The Art of Molecular Dynamics Simulation* (Cambridge University Press, Cambridge, U.K., 2004).

[34] J. E. Hacke, Jr., Am. Math. Monthly **48**, 327 (1941); see also *Handbook of Mathematical Functions With Formulas, Graphs, and Mathematical Tables*, Natl. Bur. Stand. Appl. Math. Ser. No. 55, edited by M. Abramowitz and I. A. Stegun (U.S. GPO, Washington, DC, 1972).

[35] W. H. Press, B. P. Flannery, S. A. Teukolsky, and W. T. Vetterling, *Numerical Recipes in FORTRAN*, 2nd ed. (Cambridge University Press, Cambridge, U.K., 1992).